J. Condensed Matter Nucl. Sci. 41 (2026) 189–202

Research Article

An XAFS Study on the Surface Structure After an Anomalous Heat Generation Experiment Using a Material System of Ni/Cu Multilayer on Ni Substrate

Tatsumi Hioki
Institutes of Innovation for Future Society, Nagoya University, Nagoya, Japan

Yasuhiro Iwamura, Takehiko Itoh
School of Science, Yokohama City University, Yokohama, Japan

Takehiko Itoh, Jirohta Kasagi
Research Center for Accelerator and Radioisotope Science (RARIS), Tohoku University, Sendai, Japan

Tatsumi Hioki, Shinobu Yamauchi
Previously with CLEAN PLANET Inc., Tokyo, Japan

Tomonori Takahashi
CLEAN PLANET Inc., Tokyo, Japan

Abstract

The anomalously large heat generation phenomenon using hydrogen gas and nanoscale Ni/Cu multilayer films on Ni sheets was investigated by SEM-EDX and XAFS analyses for a sample that showed significant excess heat generation during a long-term heat generation experiment. SEM observations of the sample in back scattered electron mode revealed randomly distributed dark regions of anomalously high oxygen concentration, surrounded by grey regions with only trace oxygen concentration. The dark regions corresponded to the regions of high oxygen concentration (RHOC) reported in previous studies. XAFS analyses of the sample suggested that approximately 5% of the Ni or Cu atoms in the surface layer were in a chemical state similar to oxygen-deficient $NiO_{1-\delta}$ or $CuO_{1-\delta}$, and were localized in the RHOC. It was also suggested that the RHOC extended to a depth of $\sim$0.8 μm or more which was much deeper than the initial multilayer thickness of $\sim$150 nm. If the RHOC were formed as a result of cumulative events of anomalous heat generation, then a local atomic configuration, in which a significant number of both oxygen atoms and their vacancies occupy octahedral interstitial sites adjacent to Ni atoms with a face-centered cubic structure, may be an efficient nuclear active environment for anomalous heat generation.
© 2026 ICCF. All rights reserved. ISSN 2227-3123

© 2026 ICCF. All rights reserved. ISSN 2227-3123

Keywords: Anomalous heat generation, Ni/Cu multilayer, Region of high oxygen concentration, XAFS, Oxygen deficient nickel oxide, Oxygen, Vacancy.

1. Introduction

An anomalously large heat generation phenomenon using nanoscale Ni/Cu multilayer films and hydrogen gas has been reported by Iwamura et al [1]–[6]. They prepared a material system consisting of ∼100 nm-Ni/Cu multilayers on a 100 μm-Ni substrate. When the system was preloaded with hydrogen followed by rapid evacuation of the hydrogen and simultaneous heating to several hundred °C, excess heat was triggered. Once triggered, the excess heat occurred continuously over a long period (e.g., 6 ∼ 80 h [7], [8]), sometimes accompanied by sudden bursts of heat [2]–[5], [9], [10]. This anomalously large heat generation phenomenon was also confirmed by the photon radiation calorimetry method established by Kasagi et al. [7]–[10]. The total amount of excess heat was so large that it could not be explained by known chemical reactions. This anomalously large heat generation is hypothesized to originate from nuclear-related reactions [5], [8], although direct evidence such as gamma-rays or neutrons has not been clearly observed [5]. Furthermore, no significant increase in helium-4 (^{4}He) was observed in mass spectroscopy measurements during anomalous heat generation experiments [5]. However, scanning electron microscopy (SEM) observations revealed that there were characteristic regions on the surface of the sample after the anomalous heat generation experiments, namely regions of high oxygen concentration (RHOC) [5], [6]. The RHOC were randomly distributed on the surface, and their size was ∼5 μm. The oxygen concentration within the RHOC was 10 ∼ 40 at % which was anomalously high compared to less than ∼1 at % in the normal regions around the RHOC [5]. RHOC were more pronounced in samples with larger excess heat, RHOC were therefore expected to be hot spots for anomalous heat generation. Various analytical methods have been used to clarify the origin of RHOC [5], [6], but the material aspects of RHOC, such as the chemical state of oxygen in RHOC and the extent of RHOC in the depth direction have not been fully elucidated. In this study, to further characterize the RHOC, X-ray absorption fine structure (XAFS) and SEM-EDX (energy dispersive X-ray) measurements were carried out for a sample that showed a large excess heat in an anomalous heat generation experiment.

2. Experimental

2.1. Sample Preparation for SEM-EDX and XAFS Measurements

The sample used in the present study was prepared in the same way as previously reported by Iwamura et al [1]–[6]. First, using magnetron sputter deposition, 6 layers of Ni (20 nm)/Cu (3.8 nm) bilayer were deposited on a Ni sheet with a size of 0.1 mm× 25 mm× 25 mm. The Ni sheet of purity 99.9% was obtained commercially from the Furuuchi Chemical Co. It was washed with acetone and annealed in vacuum (<10^{-4} Pa) at 900 °C for 72 h, and then washed with HNO_3/H_2O to remove impurities from the surface. After these pre-treatments, 3.8 nm-Cu and 20 nm-Ni films were repeatedly deposited on the Ni sheet by magnetron sputtering. The base pressure of the deposition chamber was 7.4×10^{-5} Pa. High purity Ar gas was supplied as the sputtering gas at a rate of 0.12 mL/s and the pressure of the chamber was 0.14 Pa during deposition. The sputtering conditions were 50 W for 82 s for Cu and 100 W for 368 s for Ni. To ensure uniform deposition, the substrate was rotated at 20 rpm. Figure 1 shows schematic cross-section of the multilayer sample to be fabricated by the magnetron sputtering deposition. The atomic ratio of Cu to Ni in the multilayer film 143 nm thick was $Cu_{0.16}$ $Ni_{0.84}$.

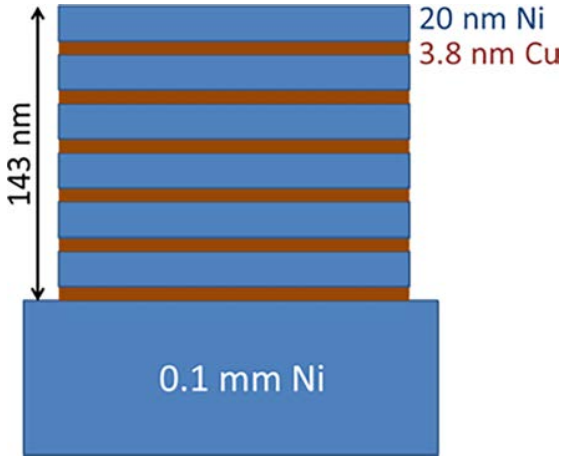


Figure 1. Schematic cross-section of the fabricated multilayer sample.

After sputtering, the multilayer sample was mounted on a sample holder in the experimental chamber for anomalous heat generation. A ceramic heater and a thermocouple were embedded in the sample holder to control the sample temperature. The experimental procedures for anomalous heat generation were as follows. First, the multilayer sample was baked for 2 days at a heater temperature of 900 °C under a vacuum of 10^{-4} Pa or less. After this baking process, the sample was cooled to 250 °C, and H_2 gas insertion into the chamber was begun. Insertion stopped when the pressure rose to 230 Pa. The pressure in the chamber then gradually decreased over time. This hydrogen absorption process took 16 h at 250 °C. After this, H_2 gas was evacuated with a turbo molecular pump, and at the same time, the sample was rapidly heated by the ceramic heater to 900 °C. These processes triggered an anomalous heat generation reaction, followed by almost constant excess heat generation for about 10 h in a vacuum of 10^{-4} Pa or less. The excess heat power was ∼5 W against a fixed heater power of 23 W. After this anomalous heat generation experiment, the sample was removed from the chamber and analyzed with SEM-EDX and XAFS. Hereafter, this sample is referred to as the AHG sample. To analyze XAFS data of the AHG sample, XAFS spectra of reference samples such as Ni-foil, NiO, $Ni(OH)_2$, NiOOH pellets, Cu-foil, CuO, Cu_2O, and $Cu(OH)_2$ pellets were measured by the transmission method. The reference samples were provided by the Aichi Synchrotron Radiation Center.

2.2. SEM-EDX Measurements

The surface morphology of the AHG sample was observed by scanning electron microscopy (SEM) and the concentration of elements in the surface layer was measured by energy dispersive X-ray (EDX) spectroscopy, using SEM-EDX apparatus JSM-6500F (JEOL) at the Electron Microscope Center, Tohoku University. Surface morphology observations were performed by secondary electron (SE) mode and backscattered electron (BE) or COMPO mode. The former mode gives information on surface irregularities, and the latter mode gives elemental composition distribution in the surface layer, i.e., regions of heavier elements appear brighter and those of lighter elements darker. The acceleration voltage for the incident electron beam was either 5 or 15 keV. Elemental concentrations were obtained at 15 keV, where the analysis depth, i.e., the effective range of the incident electron beam, was estimated to be approximately 0.6 μm for the AHG sample assuming the sample was close to pure Ni [11].

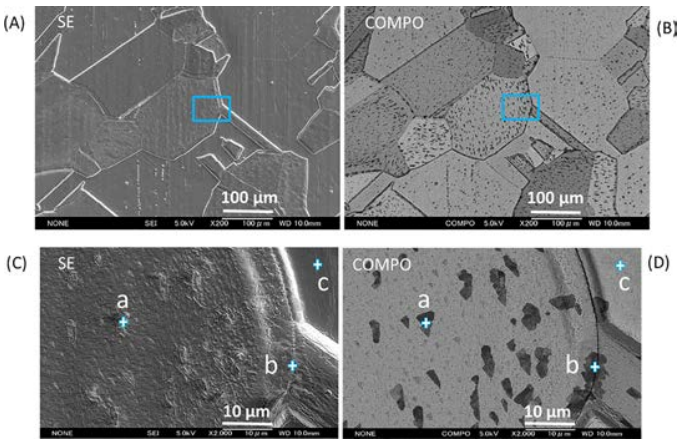


Figure 2. SEM images of the AHG sample: (A); SE image (× 200), (B); COMPO image of the same area with (A), (C); SE image (× 2000) of the blue square area in (A), (D); COMPO image of the same area with (C). These images were obtained with an acceleration voltage of 5 keV.

2.3. XAFS Measurements

To obtain information about the chemical state of the oxygen in RHOC, Ni K-edge and Cu K-edge XAFS measurements were carried out using BL5S1 at the Aichi Synchrotron Radiation Center, Aichi, Japan. The incident angle of the X-ray was fixed at 2 degrees to the sample surface to obtain information on the surface layer less than ∼1 μm thick. The size of the sample was 10 mm × 20 mm × 0.1 mm and the footprint of the incident X-ray at the center of the sample surface was 0.5 mm wide and 14 mm long. Ni K-edge XAFS was measured by the conversion electron yield (CEY) method. For this case, the analysis depth was estimated to be about 40 nm from the experimentally determined value of 41 nm for the case of Cu K-edge XAFS using Cu films with different thicknesses [12]. It should be mentioned that we could not apply the fluorescence yield (FY) method to measure Ni K-edge XAFS due to the thickness effect or the self-absorption effect [13]. Cu K-edge XAFS for the AHG sample was measured by the FY method, because Cu atoms in the AHG sample were dilute. In this case, the analysis depth was estimated to be about 0.8 μm as the depth at which incident X-ray intensity decreased to 1/e. For the reference samples, the transmission yield method was used to obtain Ni K-edge and Cu K-edge XAFS spectra. These XAFS data were analyzed using the Athena and Artemis programs [14]. X-ray absorption near edge structure (XANES) spectra were analyzed using the linear combination fitting (LCF) of the Athena program. Extended X-ray absorption fine structure (EXAFS) spectra were analyzed using the Artemis program.

3. Results

3.1. SEM-EDX Analyses

Surface morphology observation of the AHG sample was performed by SEM in both SE and COMPO modes. As shown in Figures 2(B) and 2(D), the surface had randomly distributed dark areas when viewed in the COMPO mode. This is the feature of the sample that showed an excess heat, as reported by Iwamura et al. [5], [6]. Figure 2(A) is an SE image which shows that the sample consists of grains with a size in a range from about 10 μm to a few hundred micrometers. Figure 2(B) is a COMPO image for the same area as Figure 2(A). Figure 2(B) shows that there are many dark spots randomly distributed within each grain. Figures 2(C) and 2(D) are enlarged images of the blue square area

Table 1. Concentration of elements at points a, b, and c in Figure 2(D) by SEM-EDX.

Element	Atomic concentration (at %)		
	point a (RHOC)	point b (RHOC)	point c (Normal)
O	40	32	0.90
Ni	56	62	90
Cu	∼0	0.55	0.99
C	2.7	3.5	7.8
Al	∼0	0.42	∼0
Si	0.11	0.40	∼0
Mn	0.65	0.96	∼0

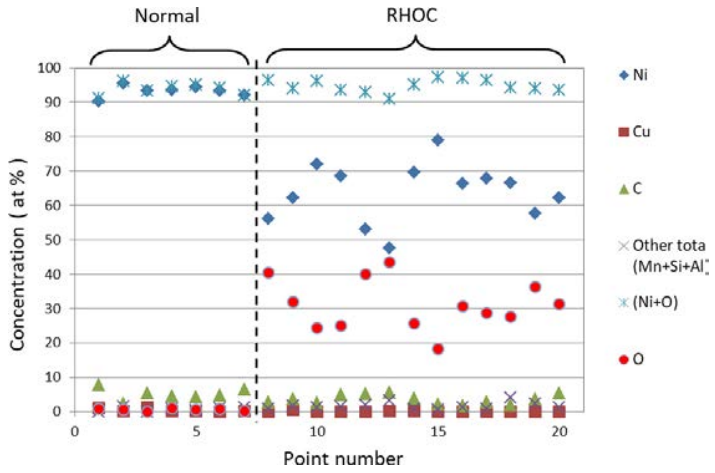


Figure 3. Elemental concentrations measured by SEM-EDX at 20 points randomly selected throughout the sample. The points a, b, and c in Figure 2 are plotted as point number 8, 9, and 1, respectively.

shown in Figure 2(A) and 2(B), respectively, and these show the same area observed in different modes. It is noted that in the COMPO images, there were many dark regions randomly distributed on the surface. The average size of the dark regions was ∼5 μm from Figure 2(D). These features of the dark regions corresponded closely to the regions of high oxygen concentration (RHOC) reported by Iwamura et al. [5], [6]. As shown in Table 1, at measurement points a and b within the dark regions in Figure 2(D), O concentrations were 40 at % and 32 at%, respectively. In contrast, at point c in a grey or normal region, O concentration was only 0.90 at%. As observed in Figure 2(C), the normal regions appear flat, whereas the RHOC resemble particles or indentations. From Figure 2(D), the total area of the dark regions (RHOC) was estimated to be roughly 10% of the total area.

As shown in Figure 2(B), dark spots were observed throughout the sample. Similar to the points a ∼ c, elemental compositions were measured at 20 randomly selected points throughout the sample; 7 points in the normal regions and 13 points in the dark regions or the RHOC. The results are shown in Figure 3, where the atomic concentrations of the detected elements O, Ni, Cu, C, Mn, Si and Al are plotted for the 20 measurement points. The concentrations of Mn, Si, and Al impurity elements are plotted as the sum of the others (Mn + Si + Al). The sum of the O and Ni concentrations (Ni + O) at each point is also plotted.

As shown in Figure 3, in the dark regions (RHOC), the O concentration varied from 20 to 45 at % depending on the measurement point. On the other hand, in the normal regions, O concentration was less than 1 at % at all points.

Table 2. Average atomic concentration for 7 normal points and 13 RHOC points (at%).

Elements	O	Ni	Cu	C	Other total (Mn+Si+Al)	Ni+O
Average of 7 points in normal regions	0.61	93	0.39	5.1	0.70	94
Average of 13 points in RHOC	31	64	0.07	3.5	1.6	95

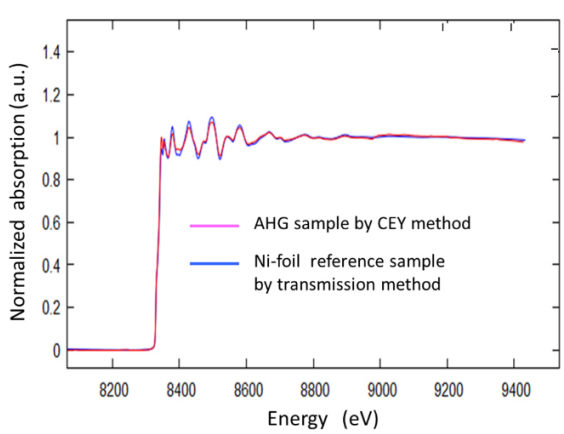


Figure 4. Ni K-edge XAFS spectra for the AHG and Ni-foil reference samples.

However, the (Ni + O) concentration at all measurement points was almost the same, at approximately 95 at%. It should be noted that several atomic percent of carbon was always detected regardless of whether it was in a normal or dark region, which was probably due to the hydrocarbons contaminated after removal of the sample from the heat generation experimental chamber to the ambient atmosphere. In addition to C, impurity elements Mn, Si, and Al were detected at low concentrations. As shown in Table 2, the average O concentration in the dark (RHOC) regions was 31 at % while that in the normal regions was 0.61 at %.

It is noteworthy that the average Cu concentration in the RHOC is much lower than that in the normal region, although the Cu concentrations in both regions are low, at less than 1 at %, which is much lower than the Cu concentration of 16 at % in the initial multilayer film. These facts suggest that Cu atoms diffused to a depth of more than $2 \sim 3$ μm into the Ni substrate, and that the Cu atoms in the RHOC, in particular, diffused deeper than in the normal regions. The latter fact suggests that the local temperature in the RHOC during the anomalous heat generation experiment was higher than in the normal regions.

3.2. XAFS Analyses

3.2.1. *Ni K-edge XAFS*

Figure 4 shows a comparison of the Ni K-edge XAFS spectrum for the AHG sample measured by the CEY method with the spectrum of a Ni-foil reference sample measured by the transmission method. The two spectra nearly overlap in the near-edge and extended structure regions, indicating that the AHG sample is close to metallic Ni. However, as shown in Figure 5, the Ni K-edge XANES spectra are slightly different between the two curves, with slight differences in the peak top energy and intensity. According to the report by Iwamura et al. [5], NiO and $Ni(OH)_2$ were

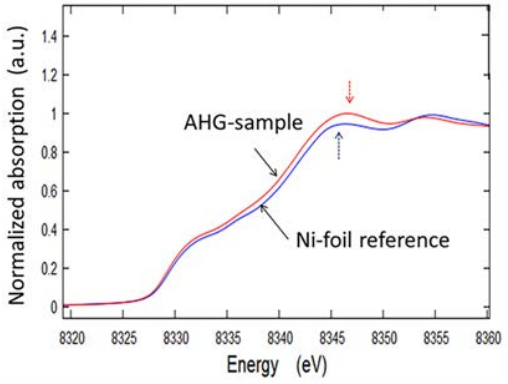


Figure 5. Ni K-edge XANES spectra for the AHG and Ni-foil reference samples.

Table 3. Results of linear combination fitting in descending order of R-factor.

Combination	**R-factor**	**A: Ni**	**B: NiO**	**C: $Ni(OH)_2$**	**D: NiOOH**
		weight: α	weight: β	weight: γ	weight: δ
A, B	0.002419	0.948187	0.051813	–	–
A, B, D	0.002505	0.931780	0.068220	–	1.445E-09
A, B, C	0.002516	0.930691	0.069309	4.724E-09	–
A, C	0.002768	0.961767	–	0.038233	–
A, C, D	0.002787	0.954165	–	0.045835	3.516E-09
A, D	0.002954	0.973061	–	–	0.026939
B	0.283693	–	1	–	–

detected on the surface of the samples after anomalous heat generation experiments using X-ray photoelectron spectroscopy (XPS), although the analysis depth of XPS was less than ∼10 nm. The NiO detected by XPS was thought to be mainly due to a native oxide layer less than a few nanometers thick [15], which was likely formed during the removal of the sample from the heat generation experimental chamber into the atmosphere required for subsequent XPS measurements. During this process, the sample was exposed to atmospheric moisture, which may have resulted in the formation of Ni(OH)2 on the surface. Therefore, we assumed that the surface layer of the AHG sample was composed of Ni, NiO, Ni(OH)2, and NiOOH and attempted to reconstruct the experimental XANES spectrum as a linear combination of these reference materials, i.e.,

$$\mathrm{X_AHG} = \alpha(\mathrm{X_ref.A}) + \beta(\mathrm{X_ref.B}) + \gamma(\mathrm{X_ref.C}) + \delta(\mathrm{X_ref.D}) \quad (1)$$

where α + β + γ + δ = 1, X_AHG is the XANES spectrum of the AHG sample, X_ref.A, X_ref.B, X_ref.C and X_ref.D are the XANES spectra of the reference samples of Ni, NiO, $Ni(OH)_2$, and NiOOH, respectively. In Figure 6, the XANES spectra of the AHG and the four reference samples are compared. A linear combination fitting of the spectra in the range from 8309 eV to 8359 eV was performed by using the Athena program. As shown in Table 3, among all combinations of the four reference materials, the combination of Ni and NiO showed the best fit (lowest R-factor).

Figure 7 compares the XANES spectrum of the AHG sample with the LCF fitted spectrum as the sum of 95% Ni_ref. and 5% NiO_ref. reference spectra. The analysis depth of the Ni K-edge XAFS by the CEY method was estimated to be approximately 40 nm, which is approximately 10 times the thickness of the native oxide film. There-

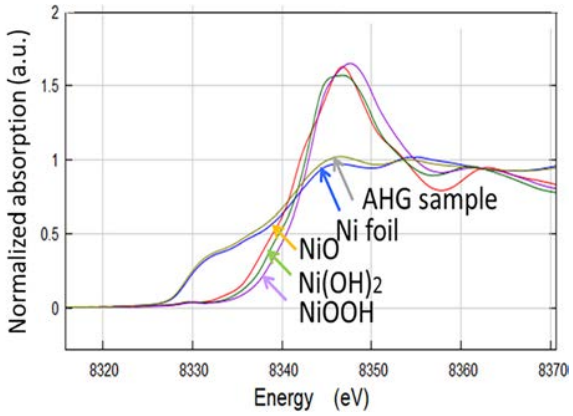


Figure 6. Ni K-edge XANES spectra for the AHG and four reference samples.

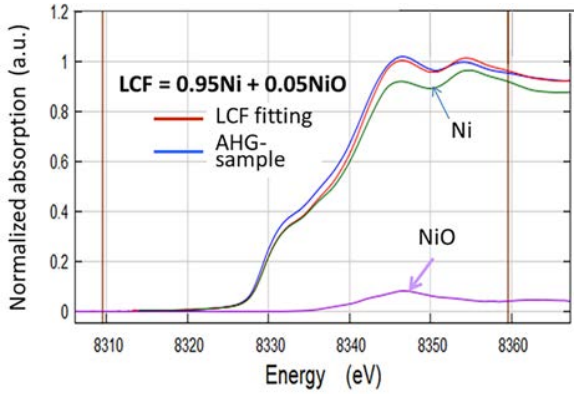


Figure 7. Ni K-edge XANES spectra of the AHG sample (blue) and the LCF fitting (red) as a sum of 95% Ni reference (green) and 5% NiO reference (purple).

fore, it was suggested that the surface layer of the AHG sample was composed of approximately 95% Ni and 5% NiO, and that the NiO extended to a depth of more than 40 nm, much deeper than the thickness of the native oxide film. Here we assume that 95% Ni and 5% NiO correspond to the normal and dark (RHOC) regions, respectively, in the COMPO-mode SEM image, as shown in Figure 8.

However, when the RHOC are stoichiometric NiO with a cubic NaCl-type crystal structure, the O concentration is always 50 at % in any RHOC. This contradicts the SEM-EDX results, which showed that the O concentration in the RHOC varied from 20 to 45 at%. Therefore, the 5% NiO component is considered to be oxygen-deficient, i.e., $NiO_{1-\delta}$. Therefore, the crystal structure of the RHOC is basically cubic NaCl-type, and the crystal structure of the normal regions is a face-centered cubic (FCC) Ni structure. It should be noted that if a $NiO_{1-\delta}$ reference sample, with $\delta = 0.57$ for example, were available, the proportion of the $NiO_{0.43}$ component would increase to more than 5%, because as δ increases, the XANES of $NiO_{1-\delta}$ approaches that of the Ni-foil reference sample.

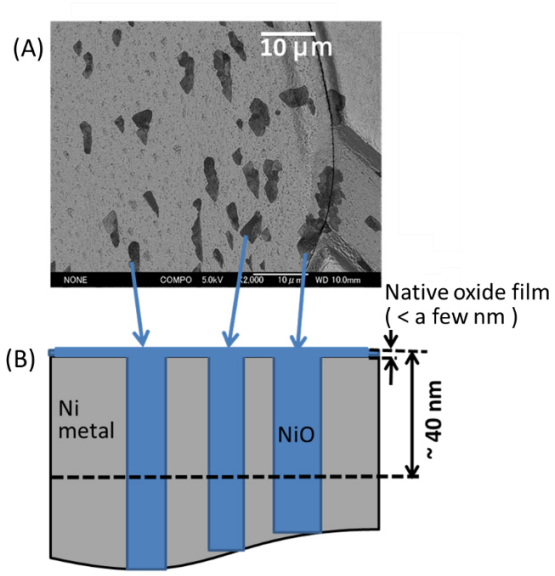


Figure 8. Possible surface layer structure of the AHG sample: (A); COMPO mode SEM image of the surface (same as Figure 2(D)), (B); schematic cross section of the dark (RHOC) regions suggested from Ni K-edge XANES analysis. Only the major elements of Ni and O are taken into account.

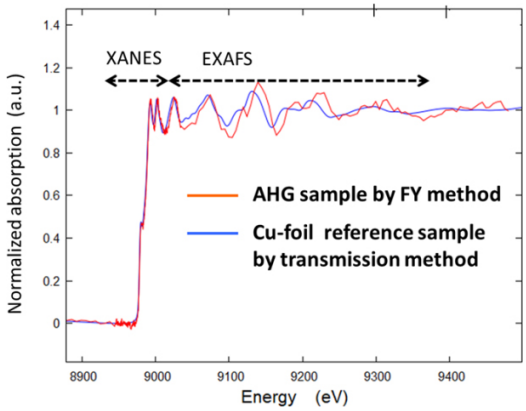


Figure 9. Comparison of Cu K-edge XAFS spectra between the AHG and Cu-foil reference samples.

3.2.2. *Cu K-edge XAFS*

As mentioned in Section 3.1, the Cu concentration in the AHG sample was less than 1 at%. Therefore, the fluorescence yield (FY) method was used for the Cu K-edge XAFS measurements. Figure 9 compares the Cu K-edge XAFS spectra of the AHG sample measured by the FY method and the Cu-foil reference sample measured by the transmission method.

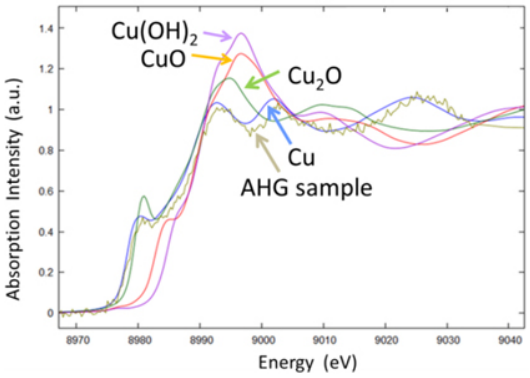


Figure 10. Cu K-edge XANES spectra for the AHG and four reference samples.

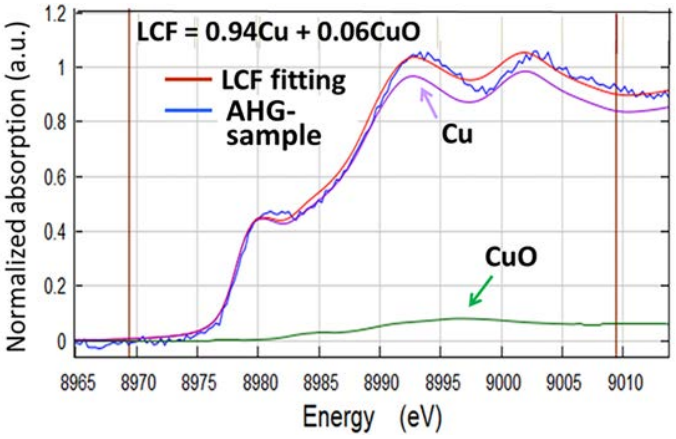


Figure 11. Cu K-edge XANES of the AHG sample (blue) and LCF fitting (red) as a sum of 94% Cu reference (purple) and 6% CuO reference (green) materials.

The two spectra are similar in the XANES region but different in the EXAFS region. The XANES region spectrum suggests that the chemical state of the Cu atoms in the AHG sample is similar to that in metallic Cu, while the EXAFS region results suggests that the environment of the Cu atom in the AHG sample is different from that in metallic Cu. The Cu K-edge XANES spectrum of the AHG sample was slightly different from that of the Cu-foil, as shown in Figure 10, which also shows the XANES spectra of the Cu-foil, CuO, Cu_2O and $Cu(OH)_2$ reference samples.

As in the case of Ni K-edge XANES, LCF fitting by the Athena program was also applied to Cu K-edge XANES using the four reference materials. Among the combinations of the reference materials, the best fit was obtained when the AHG sample was assumed to consist of 94% Cu metal and 6% CuO, as shown in Figure 11. This means that 94% and 6% of the Cu atoms in the surface layer of the AHG sample are in chemical states similar to metallic Cu and non-metallic CuO, respectively. Therefore, 94% of the Cu atoms are in the normal region and 6% of the Cu atoms are in the RHOC. Notably, 6% CuO is in close agreement with 5% NiO obtained from Ni K-edge XANES. This is natural if we consider that Cu atoms in the AHG sample would occupy the substitutional sites of Ni. The analysis

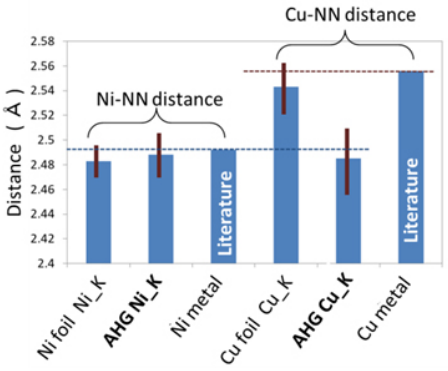


Figure 12. Comparison of experimental values of Ni-NN and Cu-NN in the AHG sample to those in the reference samples and to literature values.

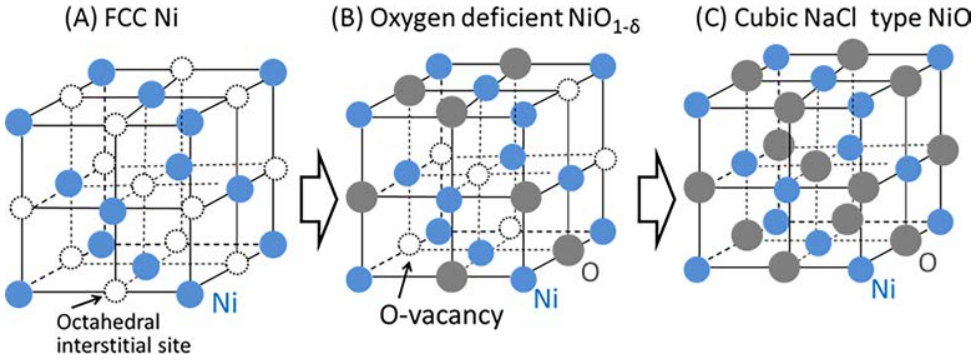


Figure 13. Comparison of crystal structures: (A) FCC Ni; (B) oxygen deficient $NiO_{1-\delta}$; (C) stoichiometric NiO. $NiO_{1-\delta}$ and NiO are formed if the octahedral interstitial sites of FCC Ni are occupied by oxygen partially and fully, respectively. In the case of (B), δ is 0.57 and O concentration (O/(Ni+O)) is 30 at %.

depth of Cu K-edge XANES by the FY method was estimated to be approximately 0.8 μm. Therefore, it is suggested that the Cu atoms in a chemical state similar to CuO extended to a depth of $\sim$0.8 μm or more. This also means that the RHOC extended to a depth of $\sim$0.8μm or more, which was much deeper than the initial Ni/Cu multilayer thickness of $\sim$150 nm.

From the Cu K-edge EXAFS spectrum of the AHG sample shown in Figure 9, the distance between a Cu atom and its nearest neighboring atom (NN), i.e., the Cu-NN distance, was determined using the Artemis program. In the analysis, it was assumed that the AHG sample had an FCC structure and the coordination number of the Cu atom was 12. The result for Cu-NN distance is shown as AHG Cu_K in Figure 12. Similarly, the distance between a Ni atom and its nearest neighboring atom, Ni-NN distance, in the AHG sample was determined from the Ni K-edge EXAFS spectrum and is shown as AHG Ni_K. In the figure, experimental values determined from EXAFS spectra of the Ni-foil and Cu-foil reference samples are also shown with literature values. In the AHG sample, the Cu-NN distance was shown to be equal to the Ni-NN distance, indicating that a small number of Cu atoms randomly occupy substitutional sites of Ni atoms, the main element that forms the FCC structure of the AHG sample.

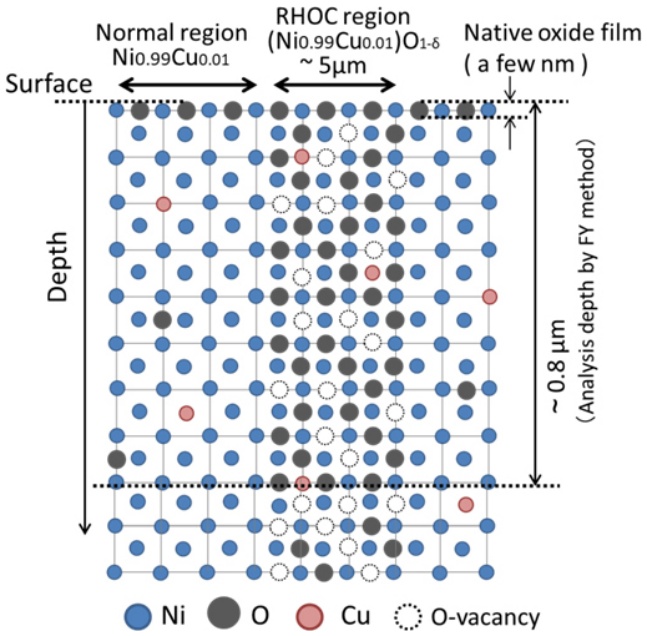


Figure 14. Schematic cross-section for the surface layer of the AHG sample. Ni atoms form FCC structure. Cu atoms of less than ∼1 at % randomly occupy the substitutional sites of Ni. O atoms in normal area are less than 1 at % and are assumed to randomly occupy octahedral interstitial sites of FCC Ni. In the RHOC region, O atoms partially occupy the octahedral interstitial sites at a high concentration in a range of 20 ∼ 45 at % and the sites unoccupied by oxygen are denoted as O-vacancy. RHOC extends to a depth of 0.8 μm or more.

4. Discussion

4.1. Surface Layer Structure of the AHG Sample

The LCF analysis for Ni K-edge XANES suggests that ∼95% of Ni atoms in the AHG sample are in a chemical state similar to metallic Ni, and the remaining ∼5% of Ni atoms are in a chemical state similar to insulating NiO. Combined with the SEM-EDX results, we assumed that 95% of the Ni atoms originate from the normal regions with an oxygen concentration of less than 1 at % and 5% of the Ni atoms originate from the RHOC with an oxygen concentration of 20 ∼ 45 at%. Stoichiometric NiO has a cubic NaCl-type structure and if the RHOC consists of NiO, O concentration in the RHOC always becomes 50 at%. This is inconsistent with the fact that O concentration in the RHOC varied, ranging from ∼20 to ∼45 at%. Therefore, the RHOC were assumed to be oxygen deficient $NiO_{1-\delta}$. It is noted that if the octahedral interstitial sites of FCC Ni are fully occupied by oxygen, the NaCl-type cubic structure of NiO is formed as shown in Figure 13. Therefore, $NiO_{1-\delta}$ is an intermediate material between metallic Ni and insulating NiO. If δ is small such as 0.2, O concentration (O/(Ni + O)) is 44 at % and the crystal structure of the RHOC is close to cubic NaCl-type structure. If δ is large, such as 0.75, O/(Ni + O) is 20 at % and the crystal structure of the RHOC is close to FCC Ni. As shown in Figure 3 and Table 2, in both regions of normal and RHOC, Cu concentrations were detected at low values of less than 1 at%, and it is suggested that the Cu atoms occupy substitutional sites of FCC Ni from the analysis of Cu K-edge EXAFS with the Artemis program. The LCF analysis for Cu K-edge XANES suggested that approximately 6% of Cu atoms within the analysis depth of ∼0.8 μm were in a chemical state similar to CuO. The value of ∼6% was approximately consistent with the value of ∼5% obtained in the LCF analysis for Ni K-edge

XANES. This fact suggests that ∼5% of Cu atoms exist in the RHOC which extends to a depth larger than ∼0.8 μm. Since the basic crystal structure is considered to be FCC Ni, the structure of the surface layer of the AHG sample is thought to be similar to the schematic picture shown in Figure 14, where impurity elements of C, Mn, Si, and Al are neglected and the area of the RHOC is tentatively assumed to be uniform in the depth direction. Actually, in the RHOC, δ-value would vary in the depth direction as well as in the horizontal direction and the boundary between the RHOC and the surrounding normal regions would be distorted.

4.2. Anomalous Heat Generation and Oxygen

The presence of the RHOC is a prominent feature of the sample that showed excess heat in the anomalous heat generation experiments using hydrogen gas and Ni/Cu multilayer films on Ni substrates. Oxygen concentration in the RHOC was anomalously high compared to that in the normal regions surrounding the RHOC. Increased concentration of O into localized regions of the RHOC is considered difficult to explain by mechanisms based on ordinary chemical reactions; small amounts of oxygen atoms in the normal region should migrate to condensate into the RHOC, and this behavior seems to violate Fick's law of diffusion at a fixed temperature. Thus, the appearance of the RHOC is considered to be related to the generation of anomalous heat that is believed to be caused by nuclear-related reactions [4], [7]. The atomic composition of the RHOC was suggested to be $(Ni_{1-x}Cu_x)O_{1-\delta}$ with $\delta = 0.2 \sim 0.8$ and $x < 0.01$. The crystal structure of the RHOC is apparently an intermediate structure between NaCl-type cubic NiO and FCC Ni. This crystal structure is formed if the octahedral interstitial sites of FCC Ni are partially occupied by oxygen. Then, the unoccupied octahedral interstitial sites can be regarded as vacancy sites of oxygen. In the case of $\delta = 0.57$ (O concentration = ∼30 at%), the atomic composition of the RHOC can be denoted as $NiO_{0.43}[V(O)]_{0.57}$, where V(O) denotes an oxygen vacancy. Ni atoms occupy the lattice sites of FCC structure and O and V(O) occupy octahedral interstitial sites of the FCC structure. V(O) may act as a hydrogen trapping site similar to the tetrahedral interstitial sites. Therefore, it is noted that in the RHOC, a significant number of both O and V(O) are adjacent to the Ni atoms, whereas in the normal regions, only V(O)'s are adjacent to the Ni atoms. Assuming that the hot spots for the anomalous heat generation are located within the RHOC, the atomic configuration consisting of adjacent Ni-O-V(O) may work as a more effective nuclear active environment than the atomic configuration consisting of only Ni-V(O).

5. Conclusions

SEM-EDX and XAFS analyses were performed with a sample after a long-term anomalous heat generation experiment using hydrogen gas and a material system of a Ni/Cu multilayer film on a Ni substrate. The sample surface exhibited randomly-distributed regions of high oxygen concentration (RHOC) surrounded by normal regions of trace oxygen concentration. The RHOC apparently extended to a depth of 0.8 μm or more, which was much deeper than the initial multilayer thickness of ∼150 nm. It also appeared that the atomic composition of the RHOC was expressed as $(Ni_{1-x}Cu_x)O_{1-\delta}$ ($x < 0.01$, $\delta = 0.2 \sim 0.8$), and the crystal structure of the RHOC was in between face-centered cubic and NaCl-type cubic structures, depending on δ-values. The δ-values varied depending on the RHOC. Even in a region of high oxygen concentration, the δ-value may vary with a horizontal position as well as with depth. The mechanism of the anomalous heat generation is not clear, but a local atomic configuration of Ni-O-V(O), where a significant number of both oxygen atoms and their vacancies occupy the octahedral interstitial sites of FCC Ni, may provide an efficient nuclear active environment for the anomalous heat generation.

Acknowledgements

The authors would like to thank Dr. S. Towata of Aichi Synchrotron Radiation Center and Prof. M. Kawasumi of Nagoya University for valuable discussions.

References

[1] Y. Iwamura, T. Itoh, M. Saito, S. Murakami, J. Kasagi, "Evidence for surface heat release reaction over nano-sized multilayer metal composite with hydrogen gas", *Proceedings of the 21st Meeting of Japan CF Research Society,* JCF21, 1–14, 2020.

[2] Y. Iwamura, T. Itoh, J. Kasagi, S. Murakami, M.Saito, "Excess energy generation using a nano-sized multilayer metal composite and hydrogen gas", *J. Condensed Matter Nucl. Sci.,* vol. 33, 1–13, 2020.

[3] Y. Iwamura, T. Itoh, T. Takahashi, S. Yamauchi, M. Saito, S. Murakami, J. Kasagi, "Energy generation using nano-sized multilayer metal composites with hydrogen gas; intentional induction of heat burst phenomenon", *Proceedings of the 22nd Meeting of Japan CF Research Society,* JCF22, 27–39, 2022.

[4] Y. Iwamura, J. Kasagi, T. Itoh, T. Takahashi, M. Saito, Y. Shibasaki, S. Murakami, "Progress in energy generation research using nano-metal with hydrogen/ deuterium gas", *J. Condensed Matter Nucl. Sci.,* vol. 36, 285–301, 2022.

[5] Y. Iwamura, T. Itoh, S. Yamauchi, T. Takahashi, "Anomalous heat generation that cannot be explained by known chemical reactions produced by nano-structured multilayer metal composites and hydrogen gas", *Jpn. J. Appl. Phys.*, vol. 63, 037001, 2024.

[6] Y. Iwamura, T. Itoh, J. Kasagi, T. Takahashi, S. Yamauchi, M. Saito, S. Murakami, T. Hioki, "Anomalous heat burst triggered by input power perturbations observed in Ni-based nanostructured thin films with hydrogen", *J. Condensed Matter Nucl. Sci.,* vol. 38, 269–286, 2024.

[7] J. Kasagi, T. Itoh, Y. Shibasaki, T. Takahashi, S. Yamauchi, Y. Iwamura, "Photon radiation calorimetry for anomalous heat generation in Ni-Cu multilayer thin film during hydrogen gas desorption", *arXiv*:2311.18347 [physics.ins-det], 2024.

[8] J. Kasagi, T. Itoh, Y. Iwamura, Y. Shibasaki, T. Takahashi, S. Yamauchi, "Photon radiation calorimetry for anomalous heat generation in NiCu multilayer thin film during hydrogen gas desorption", *J. Condensed Matter Nucl. Sci.*, vol. 39, 210–219, 2025.

[9] T. Itoh, Y. Shibasaki, T. Takahashi, M. Saito, J. Kasagi, Y. Iwamura, "Optical observation of spontaneous heat burst phenomena during hydrogen desorption from nano-sized metal composite", *J. Condensed Matter Nucl. Sci.*, vol. 36, 274–284, 2022.

[10] T. Itoh, Y. Shibasaki, J. Kasagi, S. Murakami, M. Saito, Y. Iwamura, "Optical observation on anomalous heat generation from nano-sized metal composite", *Proceedings of the 21st Meeting of Japan CF Research Society,* JCF21, 15–25, 2021.

[11] H. Soejima, "Depth resolution of electron spectroscopy analysis", *Journal of The Surface Science Society of Japan*, vol. 5, no. 3, 351–363, 1984.

[12] T. Nonaka, K. Kawase, S. Ozaki, K. Doumae, M. Takemura, A. Mikami, A. Yonetama, S. Kamimura, "Comparison of conversion electron yield and fluorescence yield methods in thin film and trace element XAFS measurements", presented at *16th Joint Symposium on Synchrotron Radiation Science at the Annual Meeting of the Japanese Society for Synchrotron Radiation Research*, 9–11 Jan 2003, Himeji, Japan, 10P11. https://sunbeam.spring8.or.jp/top/seika/ohp/JSSR2002/10P11

[13] L. Troger, D. Arvanitis, K. Baberschke, H. Michaelis, U. Grimm, E. Zscheck, "Full correction of the self-absorption in soft-fluorescence extended x-ray absorption fine structure", *Phys. Rev. B*, vol. 46, 3283–3289, 1992.

[14] B. Ravel and M. Newville, "Athena, Artemis, Hephaestus: data analysis for x–ray absorption spectroscopy using IFEFFIT", *J. Synchrotron Rad.,* vol.12, 537–541, 2005.

[15] S. Suzuki, Y. Ishikawa, M. Isshiki, Y. Waseda, "Native oxide layers formed on the surface of ultra-high-purity iron and copper investigated by angle resolved XPS", *Material Transactions, JIM,* vol. 38, 1004–1009, 1997.